revista engenharia agrícola
Journal of the Brazilian Association of Agricultural Engineering
ISSN: 1809-4430 (on-line)

WHITE MOLD DETECTION IN COMMON BEANS THROUGH LEAF REFLECTANCE SPECTROSCOPY

Doi:http://dx.doi.org/10.1590/1809-4430-Eng.Agric.v35n6p1117-1126/2015

MARLEY L. MACHADO[1], FRANCISCO DE A. C. PINTO[2], TRAZILBO J. DE PAULA JUNIOR[3], DANIEL M. DE QUEIROZ[4], OZIRES DE A. T. CERQUEIRA[5]

ABSTRACT: This study aimed to identify wavelengths based on leaf reflectance (400-1050 nm) to estimate white mold severity in common beans at different seasons. Two experiments were carried out, one during fall and another in winter. Partial Least Squares (PLS) regression was used to establish a set of wavelengths that better estimates the disease severity at a specific date. Therefore, observations were previously divided in two sub-groups. The first one (calibration) was used for model building and the second subgroup for model testing. Error measurements and correlation between measured and predicted values of disease severity index were employed to provide the best wavelengths in both seasons. The average indexes of each experiment were of 5.8% and 7.4%, which is considered low. Spectral bands ranged between blue and green, green and red, and red and infrared, being most sensitive for disease estimation. Beyond the transition ranges, other spectral regions also presented wavelengths with potential to determine the disease severity, such as red, green, and near infrared.

KEYWORDS: *Sclerotinia sclerotiorum*, PLS regression, pigments, spectrum, absorption

DETECÇÃO DE MOFO-BRANCO NO FEIJÃO COM ESPECTROSCOPIA DE REFLECTÂNCIA FOLIAR

RESUMO: Este trabalho objetivou identificar comprimentos de ondas com base na reflectância foliar (400-1050 nm), visando à estimativa da severidade do mofo-branco em cultivos de feijão para diferentes datas. Foram implantados dois experimentos em períodos de outono / inverno. Utilizou-se da regressão por Mínimos Quadrados Parciais (PLS) para a definição do conjunto de comprimentos de onda que melhor estime a severidade da doença numa determinada data. Para uso desse método, as observações foram previamente divididas em dois subgrupos: o primeiro (calibração) foi utilizado para a construção do modelo, e o segundo subgrupo, para testar o modelo definido. Medidas de Raiz do Erro Médio Quadrático (RMSE) e de correlação entre valores medidos e preditos da severidade da doença foram utilizadas para avaliar os modelos. Medidas de erro e de correlação entre valores medidos e preditos do índice de severidade da doença foram utilizadas para estabelecer os comprimentos de onda que melhor estimam a doença nas diferentes datas. O índice médio de severidade de doença em cada experimento foi de 5,8% e de 7,4%, considerados baixos. Faixas espectrais de transição entre as bandas azul e verde, entre as bandas verde e vermelha e entre as bandas vermelha e infravermelha mostraram-se mais sensíveis à estimativa da doença. Outras regiões espectrais também apresentaram comprimentos de onda com potencial para determinar a severidade da doença, tais como: o vermelho, verde e infravermelho próximo.

PALAVRAS-CHAVE: *Sclerotinias clerotiorum*, regressão PLS, pigmentos, espectro, absorção.

[1] Engº Agrimensor, Pesquisador Doutor, Dpto. de Pesquisa, Epamig/Belo Horizonte - MG, Fone: (31) 3489-5027, marley@epamig.br
[2] Engº Agrícola, Prof. Doutor, Departamento de Engenharia Agrícola, UFV/Viçosa - MG, facpinto@ufv.br
[3] Engº Agrônomo, Pesquisador Doutor, Diretoria de Operações Técnicas, Epamig/Belo Horizonte - MG, trazilbo@epamig.br
[4] Engº Agrícola, Prof. Doutor, Departamento de Engenharia Agrícola, UFV/Viçosa - MG, queiroz@ufv.br
[5] Acadêmico em Eng. de Agrimensura e Cartográfica, UFV/Viçosa - MG, ozires_lajinha@hotmail.com
Recebido pelo Conselho Editorial em: 14-4-2014
Aprovado pelo Conselho Editorial em: 26-5-2015

INTRODUCTION

White mold [*Sclerotinia sclerotiorum* (Lib.) de Bary] is a fungus that infects seeds from numerous crops that are of great economic relevance in Brazil, such as beans, soybeans, and cotton; they can therefore be considered a limiting factor in these crops' production (BOTELHO et al., 2013). In beans, it is considered one of the most destructive diseases worldwide, particularly during fall-winter seasons. The low evapotranspiration and high soil humidity, enabled by irrigation, benefit the fungal growth unlike traditional cultivation periods (PAULA JÚNIOR et al., 2010). Once climate conditions are favorable to white mold, losses of up to 100% of both bean yield and quality can occur, mainly if susceptible cultivars are used (SCHWARTZ &SINGH, 2013).

The initial symptom of white mold is plant wilt, caused by stem rotting. Subsequent symptoms likely to occur in leaves, rods, and pods and consist of water-soaked spots, followed by cottony white mycelium growth, from which comes the name "white mold" (PAULA JÚNIOR et al., 2010). Foliar diagnose would, in this case, be one of the main methods to evaluate severity. Leaf-reflectance is determined by surface properties, internal structures, and biochemical compounds' concentration and distribution within leaf inner tissues (such as nitrogen, lignin, and cellulose) (BARTON, 2012).

Regarding healthy crops, reflectance within visible spectral range (400-700 nm) is low due to high absorbance by photoactive pigments (chlorophylls, anthocyanins, and carotenoids). In contrast, reflectance in wavelengths near infrared (700-1,050 nm) is high due to air multiple spreading across cell interfaces in internal tissues (MAHLEIN et al., 2013; PRABHAKAR et al., 2013; YANG, 2010; PONZONI & SHIMABUKURO, 2009). Thus, specific wavelengths can provide useful information when monitoring reflectance spectroscopy in crops with environmental stresses. .

Data from monitoring spectroscopy can be obtained across a wide spectral range, with only minor spectral increments, normally bellow 10 nm and might result in highly correlated predictive variables (multi collinear). Therefore, regression through Partial Least Squares (PLS) is a commonly used multivariate technique that is able to deal with a small number of observations and a great one of variables, in which certain identified "noises" (acquisition imperfections) could be irrelevant and/ or redundant (TEÓFILO et al., 2009).

The aim of this study was to propose a method for white mold severity identification and quantification through the selection of wavelengths that best estimate it.

MATERIAL AND METHODS

The Agricultural Research Agency of Minas Gerais – EPAMIG implemented the experiments and helped throughout this research project performance. The trials were carried out in two areas with white mold occurrence records. One located at the experimental field "Diogo Alves de Melo" of the Federal University of Viçosa (UFV), in Viçosa - MG, Brazil (20° 46' 05" S and 42° 52' 10" W - plot central point). The other located at the experimental farm "Vale do Piranga" of the Agricultural Research Agency of Minas Gerais (EPAMIG), in Oratórios - MG, Brazil (20° 24' 24" S and 42° 49' 08" W - experiment central point). The experiments were named as UFV and FEVP, in which the planting dates were May 5 and 18 of 2011, respectively. Both experiments were kept under conventional sprinkler irrigation and planting systems. Soil preparation was carried out by a disk plow. Weeds were manually hoed, and pests were controlled by insecticide applications. We used the commercial formulation 8-28-16 of $N–P_2O_5–K_2O$ for time-of-planting fertilization. After emergence, plants received topdressings with molybdenum solution. The experimental plot was composed of five 3-m rows spaced in 0.5 m, with the four central lines comprising the useful area. The experimental design was randomized blocks with four replications. The treatments were arranged in a 4x2x2 factorial scheme, consisting of plant densities (4, 7, 10, and 13 plants.m^{-1}), upright bean genotypes of type II (CNFC 10720 and VC 6) and treatments with Fluazinam fungicide (with or without application), totaling 16 treatments. Factorial interactions were used to assist EPAMIG research objectives, considered in this study as a method of assessing the different levels of disease severity. Fluazinam was applied in doses of 0.65 L.ha^{-1}, at the beginning of

flowering and again 10 days after, using a knapsack pressurized with CO_2. Control of foliar diseases was conducted before flowering, with an Azoxystrobin compound.

The disease severity index (DSI) (%) was calculated at the R9 phenological stage (plant maturation), evaluating plants within each useful plot area individually. For this, we used a scale grid with scores ranging from 0 to 4, in which 0 = healthy plant; 1 = 1% to 25% of plants with white mold symptoms; 2 = 26% to 50% of plants with symptoms; 3 = 51% to 75% of plants with symptoms, and 4 = above 76% of plants with symptoms. Each plot DSI was calculated according to [eq. (1)] (VIEIRA et al., 2010).

$$DSI(\%) = \frac{\sum \text{score attributted to each plant}}{4 \times (\text{number of evaluated plants})} \times 100 \quad (1)$$

Reflectance readings were taken by a portable spectroradiometer (ASD FieldSpec® HandHeld 2) (Analytic Spectral Devices, Boulder, Colorado, USA) with optical sensor field of 25°, spectral range between 325-1075 nm, of 1 nm accuracy and spectral resolution lower than 3 nm in 700 nm wavelength. The adopted useful reading range was between 400 and 1050 nm (651 bands), discarding extremely noisy spectral data. Optimization operations and instrument calibration were conducted before data acquisition, using a white reference panel "Spectralon" (Labsphere, North Sutton, USA). Each reflectance point corresponded to an average of 10 scans carried out by a sensor, referring to the same target. In order to manage reflectance readings with the leaves, a contact probe with self-light source, Halogen type, 6 watts of power, with color temperature of 2911+/-10 K was used. This probe was used to eliminate undesirable spectral variations that would be enabled by the field geometry of the sensor in accordance with the leaf-surface orientation. Calibrations, using the "Spectralon" panel, were handled in intervals of 10 to 20 minutes. The halogen bulb was pre heated for 90 minutes before readings, seeking to improve spectral data quality and homogeneity (MANHALEN, 2010). The integration time for conversion of the received light into electrical signal was of 138 ms, accomplished in the optimization process. The foliar reflectances were obtained from 27 leaves in nine plants, once, for each plant, one leaf from the upper third, one from the middle third, and one from the lower third were collected. In this case, the respective reflectance readings were performed immediately after leaf extraction. The plot reflectance value was defined by the average of 27 foliar reflectance.

Most important wavelengths to establish the predictive model were chosen based on PLS regression, using 601 reflectance measures. PLS regression uses spectral decomposition of a dependent variable matrix (Y) in its *scores* (U) and *loadings* (Q); and spectral decomposition of an independent variable matrix (X) in its *scores* (T) and *loadings* (P). Thereby, there is a relation between *scores* T and U, where an angular coefficient *b* (*tan* α) can be detected between the axes, also called regression coefficient (Equation 2). The DSI (dependent variable) can be predicted according to measured reflectances (independent variables), in accordance with [eq. (3)].

$$b = \frac{U'T}{T'T} \quad (2)$$

$$Y_p = TbQ' + \varepsilon \quad (3)$$

in which,

Y_p=dependent variable to be predicted (DSI),

ε = residue vector.

In order to establish wavelengths that best represent the disease severity, initially, information were randomly divided into two groups, calibration and validation, with 70% and 30% of observations, respectively. After this, correlations between the reflectances were established at every wavelength and disease severity level, using the calibration group. Correlation absolute values were sorted in descending order. Then, independent variable subgroups were created, in

which the first subgroup corresponded to the lower correlation wavelength, and the subsequent groups were formed by the previous subgroup plus the upper correlation wavelength that still did not belong to any subgroup. Thus, the last subgroup to be designed had all wavelengths. Each subgroup underwent PLS regression and correlation calculations were established between DSI measured and predicted values. The model quality was measured according to the ratio between prediction correlation and root mean squared error (RMSE) (Equation 4). The RMSE was normalized by the ratio between the current value and the highest RMSE.

$$RMSE(\%) = \sqrt{\frac{\sum_1^n (y_i - \hat{y}_i)^2}{n}} \quad (4)$$

In which,

n = number of samples;

y_i = real value of dependent variable,

$\hat{y}_i$ = value estimated by the regression model.

For RMSE estimation in the calibration group, cross-validation strategy (*leave-one-out)* was used in the accounting of prediction errors. This process calibrates the PLS models by iteratively using all the data, except one. At each interaction, one different sample is left out from the data until every sample is left out once. Hereupon, these values left out from calibration are predicted and prediction residues are computed. The selected wavelengths were the ones that compose a model with the greatest measure quality (TEÓFILO et al. 2009).

The data used for PLS regression were pre-processed by a technique that focuses on the averages, according to [eq. (5)].

$$x_c = x - \mu(x) \quad (5)$$

In which,

x_c = variable value x focused on the average;

$\mu(x)$ = average of variable x.

The presence of outliers was checked by robust z-score statistics (DASZYKOWSKI et al., 2007), based on residues between measured and predicted values from the PLS regression (Equation 6).

$$\left| \frac{e_i - median\{e_i\}_{i=1}^n}{Q_n} \right| > C \quad (6)$$

In which,

e_i = i-umpteenth residue;

C = cut-off limit given the normal distribution (3 times the standard deviation);

n = number of observations,

Qn =scale estimator (Equation 7).

$$Q_n(y_1, \ldots, y_n) = 2.2219\{|y_i - y_j|; 1 \leq i < j \leq n\}_{(k)} \quad (7)$$

where,

$$h = \left(\left[\frac{n}{2}\right] + 1\right),$$

$$k = 0.5.h(h-1).$$

In which,

k = statistical order indicating the greatest value of Q_n calculated in accordance with the difference between residues ($y_i - y_j$) .

After defining the model, it was used in the validation subgroup observations. The correlations between measured and estimated values were then calculated with the purpose of quantifying the model significance for validation subgroup.

All the used methodology was developed in Matlab (Math Works, Natick, USA). The reflectance raw data processing was performed with the aid of ViewSpecProc software (Analytic Spectral Devices, Boulder, USA). For the PLS regression, OPS Toolbox package was used (TEÓFILO et al., 2009).

RESULTS AND DISCUSSION

Both experiments had low DSIs. In Viçosa, DSI averaged 5.8%, in which 28.1% of the plots were not infected, 67.2% were between 0.1 to 25%, and 4.7% from 25.1 to 50%. In Oratórios, DSI was 7.4%, being that 20.3% of plots were not infected, 70.3% were from 0.1 to 25%, and 9.4% between 25.1 to 50%. The majority of the plots presented a DSI below 3%, in both experiments. Leaf spectra in the two experiments showed, in the majority, differentiated performances, considering the two dates of days after emergence (DAE), before and after flowering, and DSI levels (Figure 1). Spectra before and after flowering are justified by primary infections caused by ascosporous germination in presence of free water and exogenous energy source, usually petals of senescent flowers and necrotic tissues fallen on the ground or retained in plants (PAULA JUNIOR ET AL., 2009). In the FEVP experiment (Figure 1a), there is an obvious separation between the stage before flowering (25 DAE) and the post-flowering (60 DAE), a fact that is not observed in the UFV experiment (Figure 1b). Greater reflectances of 25 DAE (Figure 1a) are due to most satisfactory crop vegetative vigor in this period. Spectra with 0% of DSI are visually discernable from the others (Figure 1a) for the ranges of green (500-600 nm) and red (600-700 nm), as well as for the near infrared (750-1050 nm) at 60 DAE. Regarding UFV (Figure 1b), spectra with 0% of DSI are visually distinguishable from the others in the near infrared range. The blue range (400-500 nm) and the majority of the *red-edge* (700-750 nm) visually performed lower difference. Therefore, for the two experiments, there are spectral ranges in each DAE that allow distinction between leaves from healthy plants and those infected by the disease.

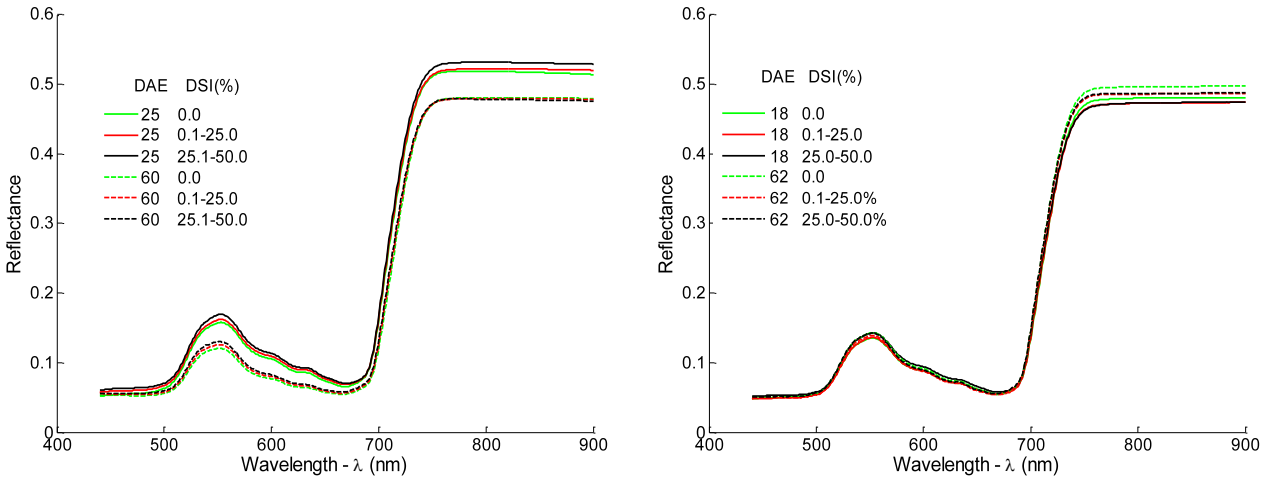

a) FEVP b) UFV

FIGURE 1. Average reflectance spectra for two dates of DAE and for DSI levels.

In spite of the low disease severity, the PLS regression of leaf reflectance exhibited possibility of white mold detection in several DAE dates during the crop cycle, even with insignificant values

of disease severity (Table 1). In all the DAE of the Calibration group, there was significant correlation (α up to 5%) among the measured and predicted DSI values. Regarding the Validation group, only in 41, 52, and 82 DAE of the FEVP experiment, the correlation was not significant. Differentiated values of degrees of freedom (DF) are due to removal of outliers.

TABLE 1. Parameters of the correlation between reflectance of wavelengths (nm) selected by the PLS regression and the disease severity index.

Exp.	DAE	Selected wavelengths (nm)					
		Calibration			Validation		
		r	RMSE	DF	r	RMSE	DF
FEVP	25	0.530***	9.07	40	0.681**	9.94	16
	41	0.372*	5.36	42	0.041ns	8.89	17
	52	0.552***	9.25	42	0.314ns	14.07	18
	60	0.510***	7.70	43	0.477*	8.01	18
	76	0.365*	5.97	42	0.558*	10.16	18
	82	0.349*	5.35	42	0.153ns	5.90	17
UFV	18	0.588**	7.36	26	0.658*	9.29	10
	34	0.553***	5.29	42	0.477*	5.39	17
	49	0.391**	8.58	45	0.669**	5.41	17
	62	0.746***	4.02	40	0.563*	5.41	17
	69	0.700***	5.59	42	0.476*	7.59	18
	83	0.692***	4.06	41	0.741***	4.16	17
	96	0.509***	5.95	42	0.687**	5.73	18

(1) Level of significance: * p<=0.05; ** p<=0.01; *** p<0.001; ns=not significant.
r: correlation measure; RMSE: Root mean squared error of prediction; DF: degrees of freedom.

The wavelengths selected by the PLS regression, considering simultaneous statistical significance in the calibration and validation groups, did not manifest a standard in the different DAEs for each experiment (Table 2).

TABLE 2. Wavelengths designated (calibration - validation) by the PLS regression with significant correlation.

Exp.	DAE	List of selected wavelengths (nm)
FEVP	25	440-606; 608-610; 678-694; 704-900;
	60	440-732; 780-900;
	76	447-700; 715-751; 756-758; 849-861; 864-864; 873-900;
UFV	18	532-533; 538-539; 542-544; 695-714;
	34	573-663; 691-692;
	49	440-552; 556-563; 566-590; 593-632; 634-634; 645-646; 650-651; 653-670; 673-674; 676-678; 702-718; 736-753; 766-900
	62	440-443; 464-464; 504-504; 506-506; 573-573; 649-723; 762-900;
	69	491-502; 505-661; 718-900;
	83	500-500; 522-523; 527-528; 533-534; 538-541; 545-725; 735-900;
	96	501-510; 512-519; 521-523; 729-900;

Based on the wavelengths displayed on Table 2, the frequency of use in models and the PLS regression coefficients of greatest value were employed in order to extract the most representative wavelengths (Table 3). The frequency was established from the number of times that each

wavelength was used in the experiments. Thus, the two greatest frequencies of wavelengths were suggested (seven and eight times).

TABLE 3. The most frequent wavelengths (λ) by using the PLS regression.

Freq.	Wavelengths (λ, nm)
7	506, 522-523, 533, 538-539, 574-590, 593-606, 608-610, 650-651, 653-661, 718, 780-848, 862-863, 865-872
8	573, 849-861, 864, 873-900

The greatest PLS regression coefficient for each DAE, obtained by the normalized *b* value (Equation 2), was used to indicate the wavelength that contributed the most for disease determination (Table 4). In this case, the regression coefficients can be positive or negative.

TABLE 4. Wavelengths (λ) with the highest PLS regression coefficient (b).

FEVP			UFV		
DAE	λ	b	DAE	λ	b
25	$504^{(+)}$	7,438.25	18	$710^{(+)}$	124,086.08
60	$532^{(+)}$	122.82	34	$663^{(+)}$	973.85
76	$715^{(+)}$	95.00	49	$752^{(+)}$	195.74
			62	$692^{(-)}$	3,152.56
			69	$509^{(+)}$	2,305.78
			83	$705^{(+)}$	35.99
			96	$517^{(-)}$	1,377.92

(+) : positive PLS regression coefficient; (-): negative PLS regression coefficient.

The difference resulted in the infrared reflectances (Figure 1) is within the normality represented by values near 0.5, starting from 760 nm. PONZONI and SHIMABUKURO (2009) reported that if reflectances were over only one leaf, fifty percent of the electromagnetic radiation incident in the near infrared would be reflected and fifty percent would be transmitted through the leaf.

Despite the low disease severity in the experiments, the PLS regression enabled determination of the wavelengths that constituted models with statistical significance and that were repeated throughout the cycle (Table 3), demonstrating therefore that these variables can interfere on the disease presence.

Table 3 proves that the infrared and the spectral ranges are the most relevant ones, due to their greater frequency over the experiments. In the green spectral range, the most representative wavelengths are of 573 nm (frequency of 8 times), together with the wavelengths of 522 to 523, 533, 538 to 539 and 574 to 590 (frequency of 7 times). This range is also represented by the wavelength of higher PLS regression coefficient (7,438.25), given by 532 nm in FEVP with 60 DAE. The disease progress promotes decreased chlorophyll concentration, causing a significant rise in reflectance in this spectral range (YANG, 2010). Other wavelengths exist in transition areas of green with ranges of blue and red, such as 506, 593 to 606 and 608 to 610 nm (frequency of seven times), as well as 504, 509 and 517 nm (greater regression coefficient in 25 DAE in FEVP, and 69 and 96 DAE in UFV, respectively). Wavelengths located in transition ranges are considered pertinent for estimations of diseases or chlorophyll. XUE & YANG (2009) defined the transition area between blue and green as *blue-edge*, similarly to *red-edge*, which would be the maximum inclination of the reflectance curve during blue and green ranges. Values in these transition bands were mentioned by HUANG et al. (2012) and MALTHUS & MADEIRA (1993), which were identified in reflectances of infected leaves (rice and Fava beans crops - *Vicia faba*, respectively).

BARTON (2012) mentioned the use of wavelengths belonging to this interval as being suitable to estimate carotenoid absorbance (especially xanthophyll) and leaf stress.

As well as the wavelengths found in the green transition range, those found in the transition from red to infrared (*red-edge*) were highly associated with the disease-infection levels of Fava beans studied by MALTHUS & MADEIRA (1993). The wavelengths related to the *red-edge*, exhibited on Table 3, were not numerous in terms of emergence frequency in the models. However, the *red-edge* was the most frequent wavelength among the greatest PLS regression coefficients. The *red-edge* corresponds to the sudden transition that takes place within the infrared visible region. Reflectance alterations in wavelengths of around 670 nm (red) induce the *red-edge* to dislocate to shorter wavelengths, which makes it a good indicator for the disease presence (SHAFRI & HAMDAN, 2009). Among the wavelengths of greater regression coefficient, the one of 692 nm at 62 DAE, in the UFV experiment, showed negative signal, while the others were positive. As the *red-edge* is a transition region between the red absorption and the infrared reflection, it acts like an inflection point between both regions of antagonistic spectral behavior. MALTHUS & MADEIRA (1993) indicated that in wavelengths near to 700 nm, a correlation transformation from positive to negative occurs between bean foliar reflectances and infection percentages caused by *Botrytis fabae*.

The red spectral range was the third most illustrative in band numbers, behind the infrared and green ones. In addition to the wavelengths existing in the transition between green and red, the interval from 653 to 661 nm revealed frequency equal to seven; and the 663 nm wavelength was the one with the greatest PLS regression coefficient, at 34 DAE in the UFV experiment. Among these wavelengths, the values of 660, 661 and 663 nm are within the limit from 660 to 680 nm cited by SIMS & GAMON (2002), that equates to the maximum absorption within the red region, and therefore are valuable for chlorophyll quantity prediction. The red spectral band radiation absorption is only accomplished by chlorophyll. Thereby, red band wavelengths in correlation with disease severity would be linked to photosynthetic pigments decrease, specially chlorophyll, that is the most predominant pigment (60%) and of greatest reflectance influence within the visible spectrum (XUE & YANG, 2009; PONZONI & SHIMABUKURO, 2009). Even though the wavelengths from 653 to 659 nm are outside the limits established by SIMS & GAMON (2002), they are adjacent of these, establishing a contiguous interval and being able to relate to chlorophyll and to disease severity.

The negative regression coefficient found in the UFV experiment at 96 DAE, 517 nm wavelength, might be associated with the same transition effect discussed for the *red-edge*, related to the UFV regression coefficient at 62 DAE. Another explanation is that the observed spectral characteristics would be more connected to senescence than to disease severity. Leaf senescence leads to decreased chlorophyll amounts which influences spectral responses within the blue and red bands; however, it affects the blue range less severely once there is a shared absorption between chlorophyll and carotenoids (MAHLEIN et al. 2013; SIMS &GAMON, 2002). Chlorophyll tends to be reduced more quickly than carotenoids when plants are under stress or during foliar senescence (GITELSON & MERZLYAK, 1994). In this case, senescence would incite reflectance increase within the visible range. Nevertheless, in the 517 nm wavelength, reflectance (absorption process) would decrease as the disease severity increases.

The infrared-range wavelengths were the ones that suggested the greatest frequency, followed by the green, considering the groups of seven and eight replications. In this case, all the wavelengths that are higher than 780 nm are disclosed. Leaf structure degradation due to disease would lessen the internal spread of electromagnetic radiation and intensify leaf transmittance within the near infrared (YANG, 2010; MALTHUS & MADEIRA, 1993). Thus, it was observed, in this study, that infrared spectral alterations, combined with the disease, occur from the 780 nm wavelength and that correspond to this range level in the spectral curve. The interval between 760 and 780 nm, which would be a curvature found between the *red-edge* inclination and the level, is not adequate for white mold estimation. This spectral range did not express wavelengths that displayed greater PLS regression coefficient for any experimental date. Accordingly, isolated

wavelengths within the visible range and of *red-edge* demonstrated to be more sensitive to white mold detection, together with the wavelengths within the infrared range above 780 nm, given the repeatability of these lengths throughout the crop cycle.

CONCLUSIONS

The wavelengths and spectral ranges described by the PLS regression were able to identify white mold, in several phenological stages, in spite of the low disease severity indexes. These wavelengths varied in accordance with the experimental area, had no pattern among the selected ones, considering all dates of DAE. This study will be able to offer more accuracy if field reflectance measures were carried out jointly with climate notes and with plant pigment quantifications, once these variables influence such reflectance values.

The spectral band transitions blue-green (*blue edge*), green-red, and red-infrared (*red-edge*) were sensitive to disease estimation. The wavelengths of 504, 506, and 509 nm were highlighted in the *blue edge*; and wavelengths of 590, 593 to 606 and 608 to 610 nm were emphasized in the transition green-red. Regarding the *red-edge*, the values of 705, 710, 715 and 718 nm were the ones that stood out.

As well as the transition ranges, other spectral regions also performed wavelengths linked to the disease severity. In the energy absorption bands, the wavelengths that stood out were 650 to 651, 653 to 661, and 663 nm for red band. The red wavelengths were located within the central part of the region, informing that the disease severity is associated with maximum absorption points within this spectral range. In regions of greater energy reflectance, wavelengths of 532 to 533 and of 538 to 539 nm were emphasized for the green band. In the infrared, the lengths that better represented disease severity were located at the reflectance-curve level (higher than 780nm). The wavelengths in the blue spectral range did not demonstrate to be good estimators for white mold severity.

ACKNOWLEDGEMENTS

The authors want to thank the Research Support Foundation of Minas Gerais state – FAPEMIG, for providing scholarships; and to the National Council for Scientific and Technological Development– CNPq for the resources that assisted this research development.

REFERENCES

BARTON, C. V. M. Advances in remote sensing of plant stress. **Plant and Soil**, Dordrecht, v.354, n.1-2, p.41-44, 2012.

BOTELHO, S.; LUIS, W.; ZANCAN, A.; MACHADO, C.; BARROCAS, E. N. Performance of common bean seeds infected by pelo fungo *Sclerotinia sclerotiorum*. **Journal of Seed Science**, Londrina, v.35, n.2, p.153-160, 2013.

DASZYKOWSKI, M.; SERNEELS, S.; KACZMAREK, K.; VANESPEN, P.; CROUX, C.; WALCZAK, B. TOMCAT: A Matlab toolbox for multivariate calibration techniques. **Chemometrics and Intelligent Laboratory Systems**, Amsterdam, v.85, n.2, p.269-277, 2007.

GITELSON, A. A.; MERZLYAK, M. N. Spectral reflectance changes associated with autumn senescence of *Aesculus hippocastanum* L. and *Acer platanoides* L. leaves-spectral features and relation to chlorophyll estimation. **Journal of Plant Physiology**, Stuttgard, v.143, p.286–292, 1994.

HUANG, J.; LIAO, H.; ZHU, Y.; SUN, J.; SUN, Q.; LIU, X. Hyperspectral detection of rice damaged by rice leaf folder (*Cnaphalocrocis medinalis*). **Computers and Electronics in Agriculture,** New York, v.82, p.100–107, 2012.

MAHLEIN, A. K.; RUMPF, T.; WELKE, P. DEHNE, H. W.; PLÜMER, L.; STEINER, U.; OERKE, E. C. Development of spectral indices for detecting and identifying plant diseases**.** **Remote Sensing of Environment**, New York, v.128, p.21-30, 2013.

MALTHUS, T. J.; MADEIRA, A. C. High resolution spectroradiometry: spectral reflectance of field bean leaves infected by *Botrytis fabae*. **Remote Sensing of Environment**, New York, v.45, n.1, p. 107-116, 1993.

PAULA JÚNIOR, T. J.; VIEIRA R. F.; LOBO JÚNIOR, M. et al. Mofo-Branco. In: Pria, M. D.; Silva, O. C. (Ed.). **Cultura do feijão**: doenças e controle. Ponta Grossa: UEPG, 2010. p.133-148.

PONZONI, F. J.; SHIMABUKURO, Y. E. Sensoriamento remoto no estudo da vegetação. São Jose dos Campos. Ed. Parêntese, 2009. 135p.

PRABHAKAR, M.; PRASAD, Y. G.; DESAI, S.; TRIRUPATHI, M. T.; GOPIKA, K.; RAO, G. R.; VENKATESWARLU, B. Hyperspectral remote sensing of yellow mosaic severity and associated pigment losses in Vigna mungo using multinomial logistic regression models. **Crop Protection**, Amsterdam, v.45, p.132-140, 2013.

SCHWARTZ, H. F.; SINGH, S. P. Breeding Common Bean for Resistance to White Mold: A Review. **Crop Science**, Madison, v.53, n.5, p.1832-1844, 2013.

SHAFRI, H. Z. M.; HAMDAN N. Hyperspectral imagery for mapping disease infection in oil palm plantation using vegetation indices and red edge techniques. **American Journal of Applied Sciences**, Vails Gate, v.6, n.6, p.1031-1035, 2009.

SIMS, D. A; GAMON, J. A. Relationships between leaf pigment content and spectral reflectance across a wide range of species, leaf structures and developmental stages. **Remote Sensing of Environment**, New York, v.81, n.2-3, p.337–354, 2002.

TEÓFILO, R. F.; MARTINS, J. P. A.; FERREIRA, M. M. C. Sorting variables by using informative vectors as a strategy for feature selection in multivariate regression. **Journal of Chemometrics**, Chichester, v.23, n.1, p.32-48, 2009.

VIEIRA, R. F.; PAULA JÚNIOR, T. J.; TEIXEIRA, H.; CARNEIRO, J. E. S. White mold management in common bean by increasing within-row distance between plants. **Plant Disease**, New York, v.94, n.3, p 361-367, mar. 2010.

XUE, L.; YANG, L. Deriving leaf chlorophyll content of green-leafy vegetables from hyperspectral reflectance. **ISPRS Journal of Photogrammetry and Remote Sensing**, New York, v.64, n.1, p.97-106, 2009.

YANG, C. M. Assessment of the severity of bacterial leaf blight in rice using canopy hyperspectral reflectance. **Precision Agriculture**, Dordrecht, v.11, p.61-81, 2010.